

Magnetic Form Factor of the Neutron*

M. R. YEARIAN AND ROBERT HOFSTADTER

Department of Physics and High-Energy Physics Laboratory, Stanford University, Stanford, California

(Received December 2, 1957)

Electron scattering from the bound neutron and proton in the deuteron has been studied at various scattering angles between 75° and 135° for 500-Mev and 600-Mev electrons. A comparison of these scattering cross sections with those of the free proton permits a determination of the density distribution of the magnetic cloud around the neutron. By using theories developed by Jankus and Blankenbecler, the root-mean-square radius of the neutron is shown to lie between the limits 0.80×10^{-13} cm and 0.90×10^{-13} cm. The choice between these radii depends on whether the deuteron total cross sections or differential (peak) cross sections are compared with the protonic scattering cross section. Since presently available theory has not yet developed sufficiently to decide definitely between these possibilities, the root-mean-square size may be taken to be $(0.85 \pm 0.10) \times 10^{-13}$ cm with small error. The neutron's magnetic cloud clearly does not have the small size obtained by measurement of its charge cloud from experiments on the neutron-electron interaction, and this anomaly challenges the present concepts of nucleon size.

I. INTRODUCTION

THIS paper is concerned with the internal magnetic structure of the neutron. Among many reasons why it is desirable to learn about this structure, we shall point to two aspects of the problem which are of current interest. The first concerns the intrinsically interesting problem of determining the neutron's internal electromagnetic features. These features are correlated with the details of the mesonic cloud in the neutron and with the question of whether there exists within it a dense core and "soft" outer cloud. Connected with this problem is the corresponding determination of the structure of the proton¹⁻³ and the question of charge independence. In most present theoretical discussions, it is usually assumed that the outer parts of the proton and neutron are identical except for the sign of the charge. This assumption is consistent with the nearly symmetrical anomalous magnetic moments of both particles. Thus it is of interest to see whether this supposition can really withstand a searching test afforded by electron-scattering methods.

A second reason for studying the neutron concerns the question of whether the deviations from point scattering, observed in the case of the proton,¹⁻³ are really structure effects or whether the deviations can be explained by a breakdown of electrodynamics.^{4,5} In the latter case, all electromagnetic structures would appear to possess a similar limiting "size" at sufficiently small distances within which such breakdown has occurred. On the other hand, if differences in the "structures" of

the neutron and proton can be detected, this observation would imply that not all of the structure or finite size effects can be ascribed to a breakdown of electrodynamics, although, of course, apparent finite size effects might still arise partially from such a breakdown. That the breakdown would be partial would appear to be unlikely, however.

For the above reasons, it appears that a direct comparison between the electron-scattering cross sections of the neutron and proton might resolve some of these questions. In the experiment to be described below, we have attempted to probe within the meson clouds of neutron and proton with electrons to examine the differences, if any, in the angular distributions of the corresponding scattered electrons. It is to be understood that we are dealing with the magnetic clouds in the two nucleons, as will appear more clearly below.

In order to make this direct comparison between neutron and proton, it is desirable to have a very large concentration of neutrons at rest in a small volume, like the protons in a corresponding gaseous target of hydrogen. Free neutrons are not available in sufficiently large numbers to form such a target. The next best solution is to use the neutron within the deuteron. The deuteron is, in fact, a very favorable nucleus for this purpose, since within it the neutron and proton are quite loosely bound. Although the nucleons are almost free, they are also in rapid motion, and this is a complication which must be taken into account. Thus the experiment we have carried out is based on incoherent scattering from the quasi-free neutron and proton of the deuteron, and the two nucleons involved have components of momentum along and opposite to the initial momentum of the incident electrons. The scattering can also be termed inelastic, since the deuteron is disintegrated in the process, the struck nucleon recoiling and shooting out of the deuteron.

The basic idea involved in the comparison has been described previously,⁶ but it will be repeated here for

* The research reported here was supported jointly by the Office of Naval Research and the U. S. Atomic Energy Commission, and by the U. S. Air Force, through the Office of Scientific Research of the Air Research and Development Command.

¹ R. Hofstadter and R. W. McAllister, *Phys. Rev.* **98**, 217 (1955).

² R. W. McAllister and R. Hofstadter, *Phys. Rev.* **102**, 851 (1956).

³ E. E. Chambers and R. Hofstadter, *Phys. Rev.* **105**, 1454 (1956).

⁴ Yennie, Lévy, and Ravenhall, *Revs. Modern Phys.* **29**, 144 (1957).

⁵ R. Hofstadter, *Revs. Modern Phys.* **28**, 214 (1956).

⁶ See reference 5, Sec. VI.

reasons of convenience: for high momentum transfers and large scattering angles, say greater than 90° , the cross section for electron scattering from a nucleon's magnetic moment is much larger than the scattering from the specific charge of the nucleon, and the charge scattering may be neglected. Under such ideal conditions, the neutron should scatter electrons with a cross section which depends only on its magnetic moment, and, since the value of the latter is well established, a comparison with the proton can readily be made. In fact, the scattering from the proton has been studied in some detail,¹⁻³ so that the distribution of magnetic density is known, at least approximately. Now if the neutron and proton have similar structures, the electron-scattering cross section of the neutron ought to be approximately one half that of the proton. This figure is obtained from the ratio of squares of the corresponding magnetic moments, $(1.91)^2/(2.79)^2=0.45$, as follows from the Rosenbluth formula for magnetic scattering.⁷ This implies that, for high momentum transfers and large angles, the cross-section ratio ought to be everywhere 0.45. On the other hand, if the neutron should have a point-structure, or a dense core, or smaller dimensions than the proton, the cross section ratio ought to exceed 0.45 by a detectable amount. Indeed, if the neutron is actually a point and the proton's size is given by the quoted experiments, namely, 0.77×10^{-13} cm, the cross-section ratio should be much larger than 0.45. In fact, the ratio should be 3.0 at 500 Mev and 135° . Such a large ratio can easily be measured and distinguished from 0.45. This was the basic motivation of the experiment.

As noted above, because the momentum transfer is high and because the deuteron's binding energy is low (2.223 Mev), the two nucleons may be considered to be free in first approximation. (This will call for further comment below.) However, as we have also pointed out, the nucleons are in motion in the deuteron. Hence we have a close analogy between our present problem and the scattering of x-rays from bound electrons in atoms when the binding energy is low. In atoms, such a process gives rise to the modified (Compton) line. The momentum distribution of the scattered electrons in the deuteron problem will appear correspondingly as a continuum with a maximum lying near the sharp scattering peak observed from a free proton. Figure 51, of reference 5, shows the type of incoherent scattering now under discussion. We may note also that the elastic scattering from the whole deuteron, i.e., the coherent scattering with respect to the two nucleons, is extremely small and not measurable under the conditions of large momentum transfer and large angles used in the present experiments.

By summing the area under the inelastic continuum of the deuteron, the cross section for the combined magnetic scattering of both the neutron and the proton

can be found. An associated measurement of the area under the free proton peak provides the comparative datum. The difference between the area of the continuum and the free proton peak area yields the cross section of the neutron at a given angle. This procedure may be carried out for several different angles of scattering, and the magnetic form factor of the neutron can thus be determined. Corrections to this simple procedure will be discussed below. A second and important method relating to the peak height of the inelastic continuum will be discussed in Sec. V(b).

II. THEORY

It may be stated at the beginning that a complete, relativistic treatment of incoherent electron scattering from the deuteron does not exist. However, certain good approximations have been worked out by Jankus⁸ and by Blankenbecler.⁹ Jankus developed a partially relativistic approximate result for the incoherent cross section at a given angle θ and incident energy E_0 , as follows:

$$\left(\frac{d\sigma}{d\Omega}\right)_d^{\text{in}} = \left(\frac{e^2}{2E_0}\right)^2 \frac{\cos^2(\theta/2)}{\sin^4(\theta/2)} \times \left(\frac{1}{1+(2E_0/Mc^2)\sin^2(\theta/2)}\right) \left\{ (1-f_d^2) + \frac{\hbar^2 q^2}{4M^2 c^2} [2(\mu_p^2 + \mu_n^2 - 3f_d^2) \tan^2(\theta/2) + \mu_p^2 + \mu_n^2 - 3f_d^2] \right\}, \quad (1)$$

$$|q| = \frac{(2p_0/\hbar) \sin(\theta/2)}{[1+(2E_0/Mc^2)\sin^2(\theta/2)]^{1/2}} = \frac{(2/\lambda) \sin(\theta/2)}{[1+(2E_0/Mc^2)\sin^2(\theta/2)]^{1/2}}, \quad (2)$$

where f_d is the deuteron's form factor, M , the mass of a nucleon, and the μ 's refer to the magnetic moments of neutron and proton. Other symbols have their well-known meanings.⁵ Equation (1) is valid¹⁰ when the momentum transfer $q > \alpha$, where $1/\alpha$ is the usual size of the deuteron ($1/\alpha = 4 \times 10^{-13}$ cm). Now, for large values of q , f_d is extremely small, and Eq. (1) becomes

$$\left(\frac{d\sigma}{d\Omega}\right)_d^{\text{in}} = \left(\frac{e^2}{2E_0}\right)^2 \frac{\cos^2(\theta/2)}{\sin^4(\theta/2)} \times \left(\frac{1}{1+(2E_0/Mc^2)\sin^2(\theta/2)}\right) \left\{ 1 + \frac{\hbar^2 q^2}{4M^2 c^2} \times [2(\mu_p^2 + \mu_n^2) \tan^2(\theta/2) + \mu_p^2 + \mu_n^2] \right\}, \quad (3)$$

⁸ V. Z. Jankus, Phys. Rev. **102**, 1586 (1956); also Ph.D. thesis, Stanford University, 1956 (unpublished).

⁹ R. Blankenbecler, Bull. Am. Phys. Soc. Ser. II, **2**, 389 (1957).

¹⁰ See reference 11, footnote 3, p. 266.

⁷ M. N. Rosenbluth, Phys. Rev. **79**, 615 (1950).

and this is essentially identical with the formulation

$$\sigma_d^{in} = \sigma_p + \sigma_n, \quad (4)$$

where σ_p and σ_n are new symbols standing for the differential cross sections of a point proton and a point neutron.

Now, if the proton and neutron have structures, our expectation might be that the same formula [Eq. (4)] would hold, except that each point cross section would have an appropriate (form factor)² multiplied into it. Blankenbecler⁹ has examined this question, allowing for the presence of structure in the nucleons, as well as for an interaction in the final state. Moreover, he used a closure rule and has avoided making some of the approximations used by Jankus.⁸ Without giving Blankenbecler's detailed result at this point, it may be stated that Eq. (4) still holds for the conditions used in this experiment, with the added modification of introducing form factors described above, except for a correction term of the order of a few percent. A discussion of Jankus' approximations and Blankenbecler's improvements will be found in Secs. 8 and 9 of a review article by Hofstadter.¹¹ We shall ignore the Blankenbecler correction in our first calculations, since it is small and presently within our experimental errors. Though small, the correction turns out to be most important in comparing the neutron size with the proton size. Hence we shall return to this important matter in Secs. IV and V. For the moment, ignoring the correction, we shall write

$$\sigma_n = \sigma_d - \sigma_p, \quad (5)$$

and this implies that a simple subtraction should provide the neutron's scattering cross section.

Expressions for σ_n and σ_p may be obtained from Rosenbluth's work.^{7,11} We may further put $F_1 \cong 0$ for the neutron,^{4,5,11} because the static charge and second moment of the charge are both zero. We therefore write for the two cross sections:

$$\sigma_n = \sigma_{NS} F_{2n}^2 \kappa_n^2 \frac{\hbar^2 q^2}{4M^2 c^2} \{2 \tan^2(\theta/2) + 1\}, \quad (6)$$

where

$$\sigma_{NS} = \left(\frac{e^2}{2E_0} \right)^2 \frac{\cos^2(\theta/2)}{\sin^4(\theta/2)} \left(\frac{1}{1 + (2E_0/Mc^2) \sin^2(\theta/2)} \right),$$

$$\kappa_n = \mu_n;$$

and

$$\sigma_p = \sigma_{NS} F_p^2 \left\{ 1 + \frac{\hbar^2 q^2}{4M^2 c^2} [2(1 + \kappa_p)^2 \tan^2(\theta/2) + \kappa_p^2] \right\}, \quad (7)$$

where $1 + \kappa_p = \mu_p$. The subscripts *NS* refer to a particle

with no spin. The ratio $R = \sigma_n / \sigma_p$ then becomes

$$R = \frac{F_{2n}^2}{F_p^2} \times \frac{(\kappa_n^2 \hbar^2 q^2 / 4M^2 c^2) [2 \tan^2(\theta/2) + 1]}{1 + (\hbar^2 q^2 / 4M^2 c^2) [2(1 + \kappa_p)^2 \tan^2(\theta/2) + \kappa_p^2]}, \quad (8)$$

from which we may extract values of the quantity F_{2n}^2 , since F_p^2 is known. The ratio R will be taken from the experimental data reported in this article. F_{2n}^2 may then be plotted as a function of angle, and it is the quantity of interest in this experiment: i.e., F_{2n} is the neutron's magnetic form factor.

It must be pointed out that mesonic exchange corrections may affect the above conclusions. For example, if an electron produces a virtual meson on one of the nucleons in the deuteron, and if it is reabsorbed by the second nucleon, an additional channel of interaction is possible, thus increasing the deuteron's inelastic cross section. We believe this effect is not a large one, but we shall return to this question later in Secs. IV and V.

III. EXPERIMENTAL RESULTS

The experimental results may be divided into four principal groups: (a) the earliest data taken with solid targets of light and heavy polyethylene (CH_2 and CD_2); (b) later data of the same sort taken with similar targets, but with more intense incident electron beams; (c) data taken with gas targets; (d) final data taken with liquid H_2 and D_2 targets.

(a) Eight independent sets of data were taken at an incident energy of 500 Mev and 135° with the polyethylene targets. The targets were matched so that they had the same numbers of protons and deuterons,

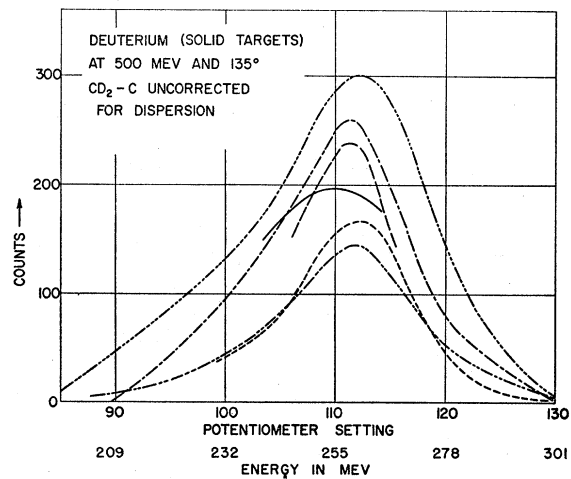


FIG. 1. Early results (six different runs) on the inelastic continuum in deuterium, obtained with solid targets of deuterated polyethylene. The abscissa is proportional to the energy of the scattered electron. The data were taken at 135° for an incident electron energy of 500 Mev.

¹¹ R. Hofstadter, *Annual Review of Nuclear Science* (Annual Reviews, Inc., Stanford, 1957), Vol. 7.

and this was checked with density measurements. For example, the data reported in Fig. 51, of reference 5, were taken with these targets. Figure 1 shows a summary of the final results obtained from some of these runs and indicates the wide spread in the heights and shapes of the inelastic continua in deuterium. The combination of statistical errors, the $\text{CH}_2\text{-C}$, $\text{CD}_2\text{-C}$ differences, and a 15% nonreproducibility of the absolute results, led to the rather large spread in the data. Similar variable results were obtained with the sharper proton peaks.

Although we shall report improved data below, we have analyzed the solid target data as indicated in Table I. This table presents the ratio of the maximum height of the free proton peak to the height of the deuterium continuum at the maximum of the latter. The half-widths of the inelastic continua were always fairly constant and averaged about 44 Mev. Although the extreme spread in this ratio varies from 7.4 to 3.2, the remaining fluctuations about the mean, 4.8, are not great. The half-widths of the proton peaks averaged 3.8 Mev for the 1% slits used in these experiments. The approximate ratio ($\sigma_d^{\text{in}}/\sigma_p$) of areas can be found by assuming triangular shapes for the peaks, as follows:

$$1 \times 44 / (4.8 \times 3.8) = 2.4 \pm 0.7.$$

Thus we may solve for σ_n , which is $(1.4 \pm 0.7)\sigma_p$ for 500 Mev at 135° . A more careful estimate, using average curves and numerical integration of the areas including the tail of the proton peak, yields the result $\sigma_n = (1.1 \pm 0.5)\sigma_p$ for 500 Mev and 135° and is about the same as the triangular mean value within the rather large error of the measurements. We shall return to the interpretation of these results later, although we may note in passing that the ratio appears to be larger than 0.45.

(b) The second set of experiments was also carried out with solid targets. These targets were cut from different sheets of CD_2 and CH_2 . At the time, operating conditions of the linear accelerator produced very large beam currents; accordingly we used currents as high as 8×10^{10} electrons per pulse (60 pulses per second). To further increase the counting rate, we used targets twice as thick as those described in the previous paragraphs. Unfortunately, the validity of the results

TABLE I. Early experimental ratios of the maximum height of the free proton peak to the height of the deuterium continuum at the maximum of the latter, for solid targets at 500 Mev, 135° .

Run No.	Peak ratio
1	7.4
2	3.2
3	4.3
4	4.4
5	4.6
6	3.7, 4.9
7	5.2
Mean	4.8

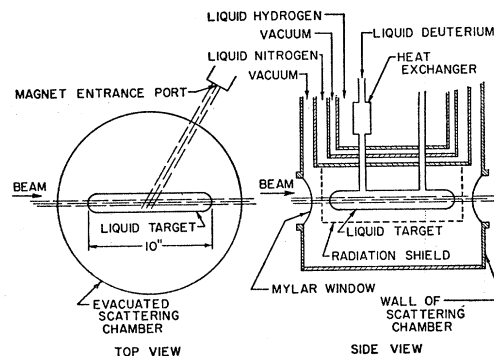


Fig. 2. Schematic diagram of the scattering arrangement and the liquid hydrogen and deuterium target.

obtained with these targets is highly questionable, since the beam currents were so intense that parts of the CD_2 targets were boiled away. This boiling occurred gradually over the period of several runs. Density measurements of samples taken at the conclusion of the runs indicated that, in the areas where the beam was concentrated most heavily, about half the deuterium atoms were missing. Now the CH_2 targets were in the beam for much less time than the CD_2 targets, because the former are used for comparison purposes and also because the counting rate in the peak is much higher. In view of the loss of deuterium, it is not surprising that the value of σ_n/σ_p at 135° fell from 1.1 to as low as 0.5 and even 0.3 for the runs during this phase of the experiment. We feel that the data from these runs are unreliable and hence these results will not be considered in the remainder of this paper. One of the curves, taken under these conditions, is shown in the *Proceedings of the Seventh Annual Rochester Conference*.¹²

(c) The advantages to be gained from using a target that has no carbon background are obvious. We therefore took one check run (at 500 Mev and 135°), using deuterium and hydrogen gases at 2000 psi as targets. The gas-target system used has been described in previous papers.^{2,5} Since only one run with gas targets has been carried out and since the counting rates are necessarily lower than they are for solid targets, the statistics are not too good; however, the absence of the carbon background makes up for this. The value for σ_n/σ_p , obtained from this run, is 1.0 ± 0.3 at 500 Mev and 135° .

(d) The most reliable data were obtained with the liquid-deuterium and liquid-hydrogen targets. The data are more reliable because the difficulty with the carbon background is eliminated without loss of counting rate. In Fig. 2 we have shown the essential details of the liquid target in a schematic fashion. This target was designed by J. A. McIntyre. The diagrams are roughly to scale, and the walls are made of stainless steel of

¹² *Proceedings of the Seventh Annual Rochester Conference on High-Energy Nuclear Physics, 1957* (Interscience Publishers, Inc., New York, 1957).

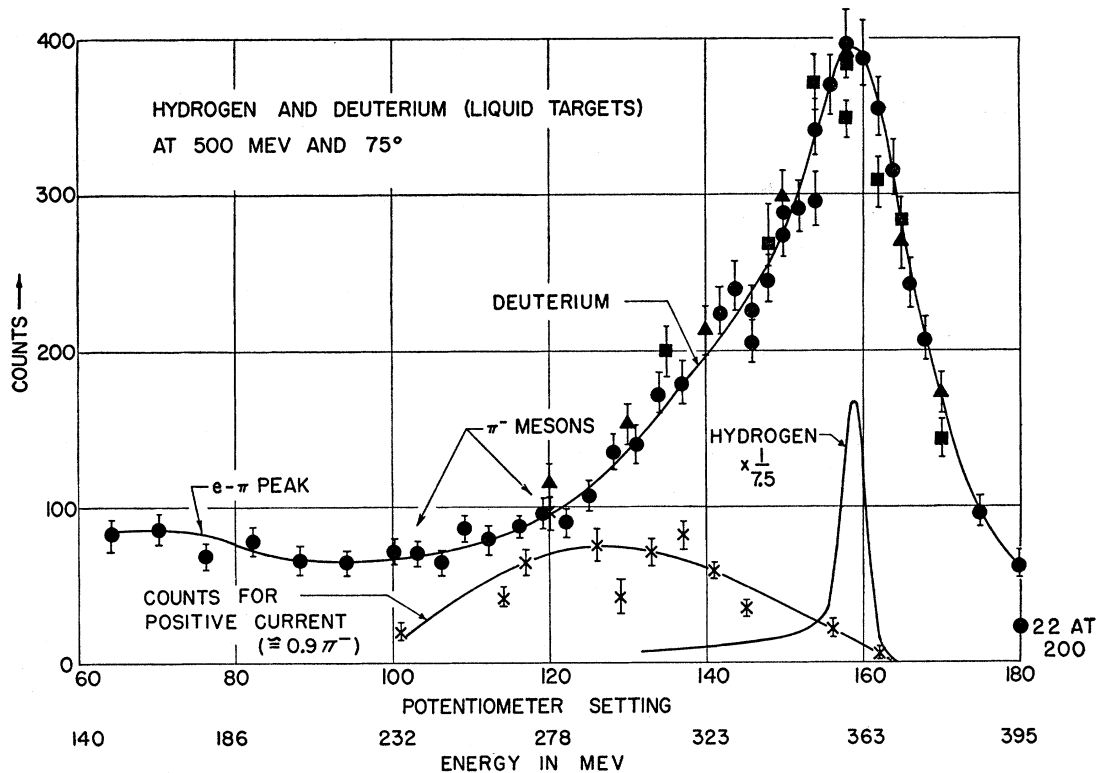


FIG. 3. The inelastic continuum at 500 Mev at a scattering angle of 75° . The large peak to the right corresponds to inelastic scattering from the moving neutron and proton in the deuteron. A negative pion contamination is indicated (" π^- mesons" in the figure). This contamination is eliminated by measurement of the positive pion yield, shown by crosses and a knowledge of the π^-/π^+ ratio. The peak, labeled " $e-\pi$," corresponds to electrons scattered after producing pions and consists also of a background of other low-energy electrons. The free proton peak is also shown. The solid circles, triangles, and squares refer to three runs. The deuteron curve should be multiplied by 0.87 to allow for the different densities of liquid deuterium and liquid hydrogen.

thickness 4 mils. In Figs. 3 and 4, we have shown two typical runs taken with the liquid target; the corrections indicated there, are discussed in the next section.

In all, ten runs have been taken with the liquid target, and the data are superior to the solid- and gas-target data. The remainder of this paper will be devoted almost entirely to the results from these liquid-target runs.

Before proceeding to a discussion of the various corrections applied to the data, we wish to report briefly our observations on the angular distribution of electrons scattered from free protons. In the original work on the structure of the proton at 500 Mev, Chambers and Hofstadter³ report for the ratio of $\sigma_p(500 \text{ Mev}, 75^\circ)$ to $\sigma_p(500 \text{ Mev}, 135^\circ)$ a value of 10.0 ± 1.0 . Our observations with the liquid targets yield a value of about 13.0 ± 1.0 for the same ratio. The geometry of the liquid targets is less favorable than that of the solid targets, since the former constitute quite broad sources of scattered electrons, and multiple-scattering losses become appreciable. To explain this discrepancy we have carried out experiments with a liquid target of hydrogen, placing a radiator in the path

of the scattered electrons to simulate conditions in the actual target. We have shown that the above difference is due to multiple-scattering losses at the edges of the region seen by the spectrometer window. This type of loss does not occur with a source of small dimensions, such as a solid target of Chambers and Hofstadter. The multiple-scattering losses are larger at 135° than they are at 75° , because the scattered energy in the former case is 260 Mev, while it is 360 Mev for the latter scattering angle. The discrepancy has thus been explained satisfactorily and quantitatively, and the proton data for the liquid target can be corrected by using the more accurate values of Chambers and Hofstadter.³ The discrepancy between liquid- and solid-target data does not affect our results on the neutron, which we shall report, since we always measure the *ratio* of the deuteron to proton cross sections and the discrepancy noted above cancels out. Any small residual error from this cause, not quite canceling out, would be well within our present experimental limits of error. This type of discrepancy may be of interest to future investigators who employ liquid targets and scattering geometry of the kinds used in this experiment.

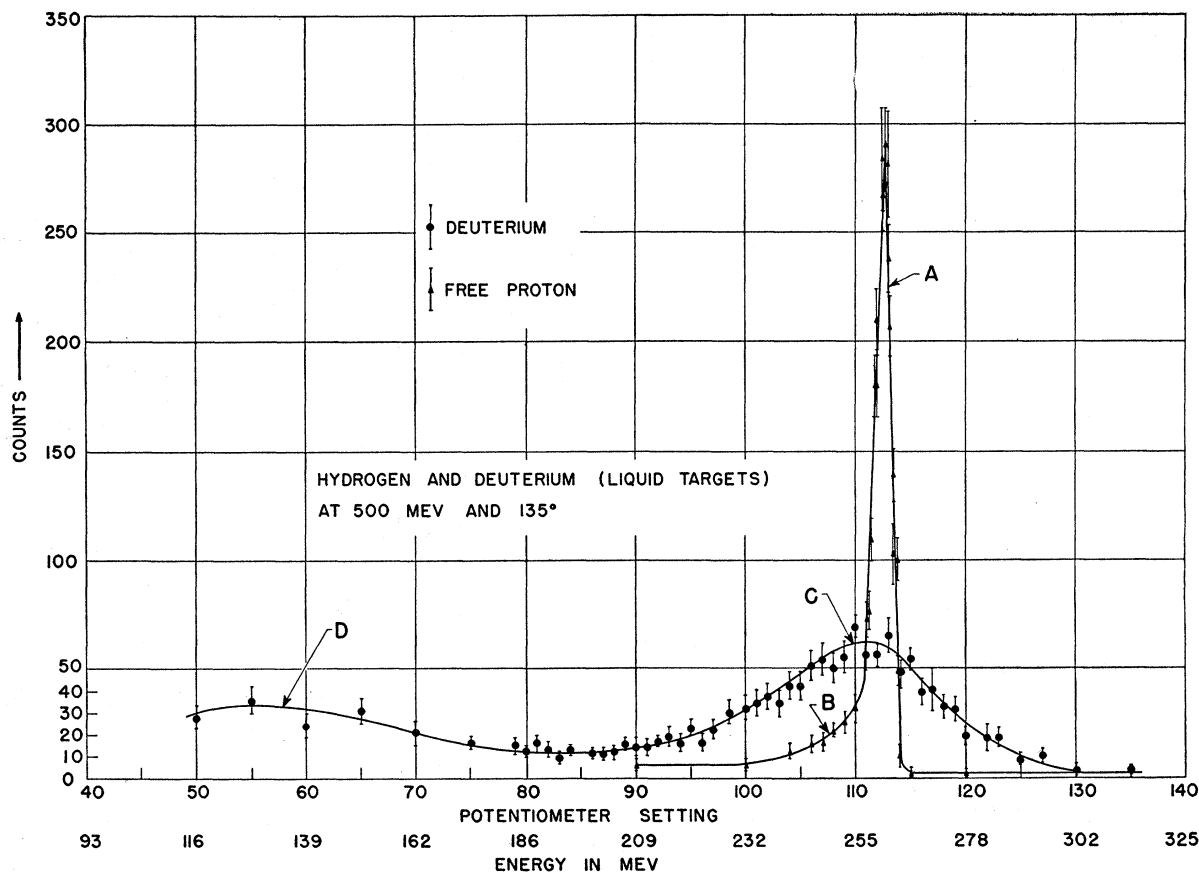


FIG. 4. A comparison of the inelastic scattering from the moving proton and neutron in the deuteron (C) and the elastic scattering of electrons from free protons (A). The data were observed at 500 Mev at a laboratory scattering angle of 135° . (D) represents the electron-pion peak and other low-energy electrons. The π^- contamination at 135° is negligible. The cross section for the neutron's magnetic scattering can be found from a comparison of the areas under the deuteron and proton peaks. The deuteron curve should be multiplied by 0.87 to allow for the different densities of liquid deuterium and liquid hydrogen.

IV. HANDLING OF THE DATA

Most early data were taken at 500 Mev and a scattering angle of 135° . With the liquid target, we have been able to take an angular distribution during a single run. At present we have investigated in detail one bombarding energy—namely, 500 Mev. We have studied the inelastic deuterium spectrum at five angles and the corresponding elastic proton spectrum at three angles at the same energy. It is not necessary to take the proton peak at all angles, since the proton's angular distribution is known.³ We have also made one run at a higher energy, 600 Mev, and at scattering angle, 135° .

On inspection of the deuterium data, we discovered that the width of the inelastic deuterium peak at half-maximum is very nearly constant at different scattering angles. The width is approximately 44–48 Mev. This can be most easily seen by sliding the peaks (Fig. 5, taken at various angles) along the energy abscissa until the peak in question corresponds to the one at, say, 75° , and normalizing the ordinates to the same value at the maximum of the peak. It is then seen that the curves

at all five angles nearly superimpose (Fig. 5) upon each other.

The similarity of the deuterium curves at different values of the momentum transfer can be of value in making the analysis of the data simpler. The simplification depends on the fact that we may now use a "standard" shape of the curve which can apply at any scattering angle. This is useful, because at different scattering angles different physical processes contribute to the background. For example, in addition to a direct pion yield coming through the spectrometer,^{13,14} there is a contribution to the background from electrons that are scattered at the angle θ after having made a pion. The peak due to this process occurs at lower energies than the inelastic deuterium peak because of the energy required to produce a pion. In general, the cross section for inelastic deuteron scattering without pion production falls essentially to zero before the above process

¹³ See reference 5, Sec. IV-c and Fig. 23.

¹⁴ R. Hofstadter, *Proceedings of the CERN Symposium on High-Energy Accelerators and Pion Physics, Geneva, 1956* (European Organization of Nuclear Research, Geneva, 1956), Vol. 2, p. 75.

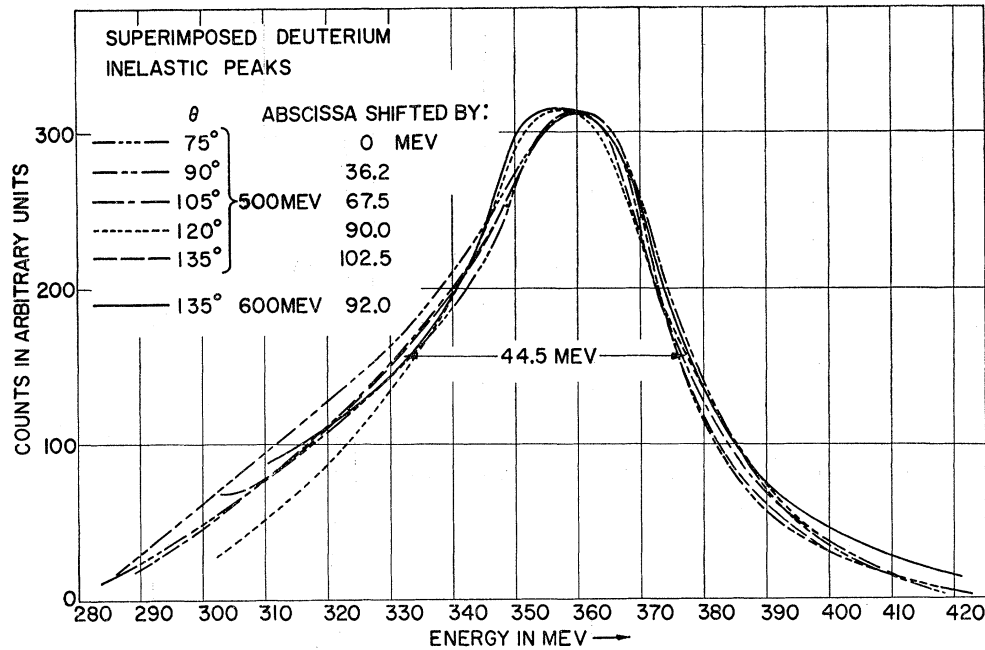


FIG. 5. The experimental spectra at five angles at 500 Mev and at 135° and 600 Mev. Within present experimental error, all curves are very similar and have equal half-widths approximating 45 Mev. Theory indicates that this behavior is to be expected. (See Fig. 7.)

becomes important, but at high values of q , say, at 135°, the two peaks begin to overlap. This can be seen in Figs. 3 and 4. (See also Fig. 12.) On the other hand, the direct negative pion background coming through the spectrometer magnet is important only at the lower q values. Thus, since the correct shape of the deuterium spectrum is known, both effects can be subtracted out, at least approximately.

These expectations have been confirmed at several scattering angles by examining the positive pion yield. Since the π^+/π^- ratio is known from the work of Sands *et al.*¹⁵ and Watson *et al.*,¹⁶ it is possible to find the negative pion yield from the measurement of the positive pion yield. The negative pion yield can then be subtracted from the inelastic spectrum. When this is done, good agreement is obtained between the resulting curve and the shape deduced from scattering angles where the pions do not contribute. The presence of the pions is indicated in Fig. 3.

We have had little hesitation in making these subtractions except in the vicinity of the extreme low-energy region of the spectrum, where the counting rates are low and the competing processes are most important. But, even in this region, the detailed shape of the curve can be found by another technique (see below).

In addition to the above subtractions, a standard instrumental correction is made. All curves must be corrected for the dispersion of the spectrometer. That is, since the width of the slits of the magnet is held fixed, the ordinates of the curves must be multiplied by a factor proportional to $1/E$.

¹⁵ Sands, Teasdale, and Walker, *Phys. Rev.* **95**, 592 (1954).

¹⁶ Watson, Keck, Tollestrup, and Walker, *Phys. Rev.* **101**, 1159 (1956).

A normalization has been made to allow for the different atomic densities of liquid deuterium and liquid hydrogen in the target.

Finally, a standard geometrical allowance has been made whenever cross sections, taken at different θ , have been compared because of varying target length in the beam. This amounts simply to multiplying the cross sections by $\sin\theta$.

In addition to the care involved in measuring the deuteron peak, considerable care is also required in handling the low-energy tail of the *proton* peak. The tail comes down rapidly at first, then falls to zero very slowly. Because the tail falls off so slowly, it comprises about 25% of the total area under the curve. Thus it is important to know the area under the tail as accurately as possible. If the tail were due entirely to bremsstrahlung, then it should be fairly simple to analyze. That is, we would expect it to decrease approximately as $1/(E-E_0')$, where E_0' is the energy at the peak. However, this seems not to be the case, presumably because of a small background. Since the counting rates are very low in the tail, the statistics are poor, and hence the tail is difficult to determine experimentally. There is undoubtedly some contribution from background effects such as wide-angle bremsstrahlung, pair-production, etc.

By using the radiative and straggling corrections,^{5,17} we may estimate how much of the tail we are missing in measuring down to a certain energy from the peak. It is then not necessary to measure the tail at energies where the background is almost the whole effect we desire to know. If we cut off the measured curve (500

¹⁷ J. Schwinger, *Phys. Rev.* **75**, 898 (1949).

Mev and 135°) at, say, 4.5% of the value at the peak, the part we are missing is calculated to be approximately 12.5% for the Schwinger correction and 12.5% for the radiative straggling in the target. Similar corrections can be applied to the inelastic deuteron peak. In this case, the curve can be measured rather well down to 33% of the peak, so that the amount missed is much smaller. In this case, we calculate the amount missed to be 8.0%. Corrections for other scattering angles are approximately the same.

We have extended the measurements in the proton tail as far as 50 Mev from the peak and have extrapolated this curve to zero counting rate. We have compared the area so obtained with the calculated missing part. In most cases the calculated values agree with the measured areas within 5%. Occasionally we have observed as much as a 10% difference. The calculated values are always less than the measured values, thus indicating a small background, probably due to wide-angle pairs, etc. We consider the proton peaks to be reasonably well measured.

In the case of the deuteron peak, we have approached the problem of the empirical shape of the peak in the following way: we shall think of the deuteron spectrum as consisting of the scattering from many little displaced proton (or neutron) peaks folded together, since the proton (or neutron) is moving in the deuteron. We have taken our most reliable proton curve (75°) and divided it into 20 small, similar proton curves; then we have folded the small peaks together again in an "empirical distribution," to see if we could reproduce the shape of the deuteron spectrum. Using this procedure, we have been successful in finding a distribution that will fit the entire curve except for the extreme low-energy end of the spectrum. Since this is exactly the place where we have experienced difficulties in subtracting out the background, we believe that our *folded* distribution

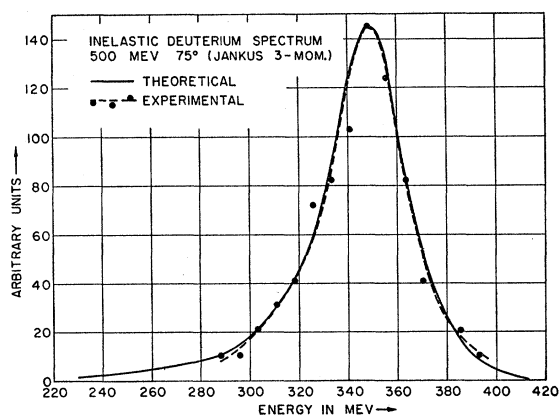


FIG. 6. The theoretical shape of the electrodisintegration spectrum at 75° and 500 Mev, according to the point-nucleon, three-momentum transfer, theory of Jankus. The experimental (unfolded) curve is also shown for comparison. The experimental curve is shifted to lower energy by 8 Mev to make the peak positions coincide.

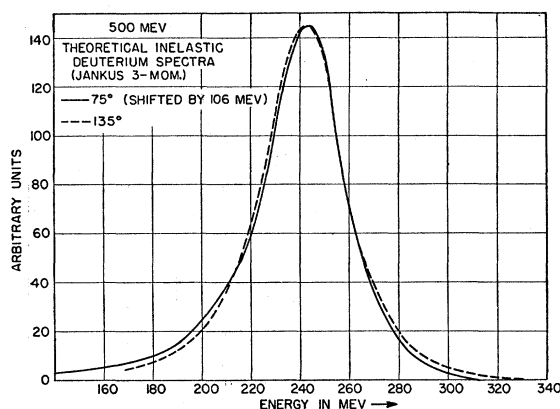


FIG. 7. This figure shows a comparison between the Jankus three-momentum, point-nucleon curves for 75° and 135° at 500 Mev. The two curves are very similar and have nearly equal half-widths.

gives us the exact shape of the lowest energy part of the actual deuteron curve. Upon comparing these results with the corresponding part of the experimental curve previously corrected for background, we find that the areas under the two curves are exactly the same. This procedure serves to convince us that (for instance) our method of subtracting mesons is substantially correct. Thus the shape of the *entire* spectrum (at any of the five angles) is known fairly well.

The above procedure was carried out and gave us an "empirical distribution" shape for the inelastic electron spectrum in the deuteron. We shall refer to this as the "unfolded" deuteron spectrum, since radiative effects have been removed (unfolded) by our calculations. This procedure resulted in a standard (for various scattering angles) deuteron spectrum yielded by our measurements.

The unfolded curve was prepared at a time before a comparison was made with theory. We shall now see that the result is in good agreement with theory. It is clear that because bremsstrahlung has been removed the unfolded spectrum is the shape to be compared with theory. Fortunately, a theory for the inelastic spectrum exists and has been given by Jankus.⁸ It was worked out, of course, for a deuteron composed of point-nucleons.

The results of the Jankus⁸ theory are given in his Eqs. (9), (10), and (11). For finite nucleons the same equations were also used (see below), but appropriate values of the nucleons' form factors were inserted in the proper places. We have computed the Jankus cross section at 75° and 135° at 500 Mev. Figures 6 and 7 show the spectra so obtained. It may be seen in Fig. 7 that, just as indicated by experiment, the shapes are very closely the same at these widely different angles. Furthermore, Fig. 6 shows the comparison between the unfolded curve, derived from our measurements at 75° , and the theoretical distribution of Jankus. The agreement is really very good. The width at half maximum

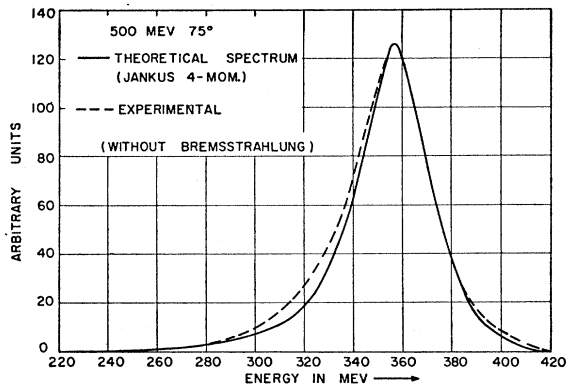


FIG. 8. The Jankus four-momentum, point-nucleon spectrum for 75° at 500 Mev in comparison with the experimental unfolded curve, i.e., the experimental spectrum with the effect of bremsstrahlung removed. The peak of the theoretical curve occurs at exactly the same energy as the peak of the experimental curve.

and shape are just as we have found experimentally. The good agreement between experiment and theory at all angles in the complicated matter of the shape of the inelastic spectrum convinces us that the Jankus theory is basically correct at the large momentum transfers even though it was designed for smaller values of q . The circumstances that the Jankus theory applies to point-nucleons, whereas the deuteron is really made of nucleons of finite size, is discussed in detail in Sec. V.

The shape of the inelastic spectrum, given in Figs. 6 and 7, thus is merely a reflection, or a transform of the momentum distribution within the deuteron. The influence of the final-state interaction has been considered by Jankus,⁸ but, at the large momentum transfer considered in these experiments, its effect is very small.

A close inspection of the positions of the peaks in Figs. 6 and 7 shows that they are shifted in the direction of lower energies by 8 and 17 Mev with respect to the actual measured peak positions at 75° and 135° , respectively. Although these shifts are not large ($\sim 5\%$), they lie outside experimental error. We have therefore sought an explanation of these shifts.

It may be observed that Jankus' results do not reduce exactly to Rosenbluth's formulas at high energy, because Jankus uses the three-momentum transfer in his theory, whereas the Rosenbluth calculation employs the relativistically correct four-momentum transfer q_μ . [The three- and four-momentum magnitudes are called s and q , respectively, in reference 11, Eqs. (1) and (8).] By substituting the four-momentum transfer in Jankus' Eq. (10), as suggested in reference 11, the Jankus result will then reduce to the Rosenbluth formula, with almost negligible differences. The calculations involved in Jankus' Eq. (10) were also carried out with the four-momentum transfer q_μ instead of the space-momentum transfer. The results were gratifying since they yielded peaks in exactly the correct positions found by experiment. The curves are shown in Figs. 8 and 9. Although the positions of the peaks are now correct, the shapes

of the curves are changed slightly compared with the three-momentum curves. At 75° the change is very small, but at 135° the four-momentum transfer curve becomes narrower by approximately 23%. Thus by changing to the four-momentum transfer, the kinematical fit is certainly improved, and the fit of the shape factor is made slightly poorer, but still quite good, considering how little is now known about the relativistic deuteron problem. It is to be noted that the 135° experimental curve is a little broader on the low-energy side than the Jankus curve with the four-momentum substitution.

We have also compared the area under Jankus' four-momentum curves, Figs. 8 and 9, with the more exact closure calculations of Blankenbecler.⁹ The results for the integrated cross sections, without final-state interaction, may be expressed as follows:

$$\sigma_d^{\text{in}} = (1 + \Delta)(\sigma_p + \sigma_n), \quad (9)$$

where σ_p and σ_n are given in Eqs. (6) and (7). For point nucleons in the Jankus theory, with four-momentum transfer, Δ is found to be $+0.02$ for 75° and -0.04 for 135° . On the other hand, Blankenbecler finds $\Delta = -0.006$ for 135° and 0.000 for 75° for point nucleons. This agreement is considered to be very satisfactory, since the corrections are so small.

Now the effect of the finite-size form factors and the interaction in the final state must be allowed for. These corrections are given for the total cross section by Blankenbecler as $\Delta = +0.03$ for 135° and $\Delta = +0.004$ for 75° with corresponding values in between these extreme angles. Thus we may use the corrected formula (9) instead of the simpler, but less exact, formula given in Eq. (4). We note, however, that no correction has been made for the meson exchange effects in the inelastic spectrum. These have been described at the end of Sec. 2 and were considered by Jankus⁸ at lower q values, where they were found to be negligible. Drell and

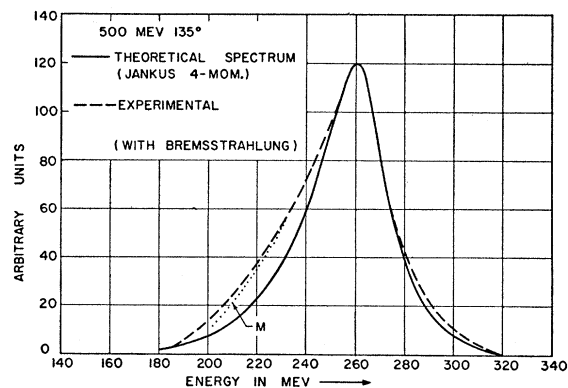


FIG. 9. The Jankus four-momentum, point-nucleon spectrum for 135° at 500 Mev in comparison with the experimental curve with bremsstrahlung included. The dotted curve, labeled M , indicates the experimental curve when corrected for the slight contribution of $(e-\pi)$ electrons. (See text and Fig. 12.)

Blankenbecler¹⁸ are now working out a more accurate estimate of this correction, but, from the good agreement between our results and the Jankus theory, the resulting correction is expected to be small.

On carrying out the integration under the experimental deuteron inelastic and proton elastic peaks and applying the various corrections that we have described above, we have found the experimental σ_d^{in} and σ_p points shown in Fig. 10. These points are the ones found directly from the liquid target data. As we have seen, the liquid target points fall off a little too rapidly at the large angles because of the multiple scattering errors. For this reason we have labeled the ordinate in Fig. 10 "approximate differential cross section." As remarked before, the ratio $\sigma_d^{\text{in}}/\sigma_p$ is independent of such errors. Table II shows the measured values. Figure 11 now presents the σ_d^{in} and σ_p values when normalized to the Chambers-Hofstadter results for σ_p . The differences between Figs. 10 and 11 are seen to be slight.

Finally we wish to show in Fig. 12 the relation between the inelastic electron-pion peak and the tail of the ordinary deuteron electrodisintegration continuum. The electron-pion peak has been calculated¹⁹ at 500 Mev and 135° from the results of the Dalitz-

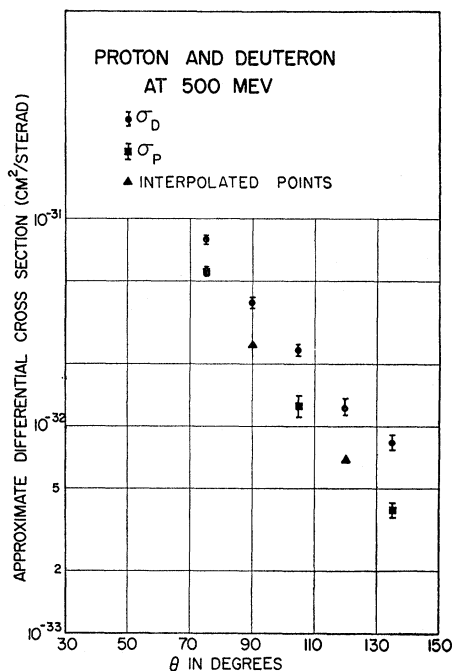


FIG. 10. The total cross section, σ_d^{in} and σ_p , are shown as obtained in this experiment. The triangles are interpolated. The cross sections are considered to be approximate on an absolute scale because multiple scattering corrections have not yet been applied. (See Fig. 11.) The deuteron cross sections should be multiplied by 0.87 to allow for the different densities of liquid deuterium and liquid hydrogen.

¹⁸ S. Drell and R. Blankenbecler (private communication).

¹⁹ We wish to thank Professor R. H. Dalitz for making the calculations for the proton at our experimental conditions.

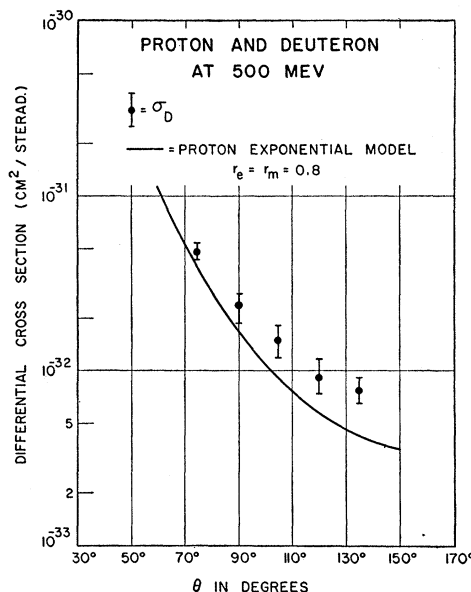


FIG. 11. This figure is similar to Fig. 10 except that the proton cross sections are corrected for multiple scattering and fit the earlier results of Chambers and Hofstadter.³ Since the ratios are not affected by multiple scattering, the ratios σ_d/σ_p in Figs. 10 and 11 are identical, except that the density factor has been included here.

Yennie²⁰ theory with the proton form factor inserted from the results of Chambers and Hofstadter.³ We have used the same form factor for the neutron and have folded the deuteron momentum spectrum into the electron-pion results. Since the deuteron spectrum is narrow compared to the electron-pion peak, the effect of the folding does not differ much from the original electron-pion peak. In any event, it can be seen that there is fortunately only a small effect (of the order of a few percent, in the worst case of 135°) of the electron-pion peak on the narrow deuteron peak we have investigated (135°), and that the effect at all other angles is smaller. The actual experimental overlapping is a little larger than calculated in the above way, and this is attributable to wide-angle pairs, Dalitz pairs, pairs from neutral pions, etc. The fortunate circumstance that the overlapping is small makes experiments of this type possible.

V. ANALYSIS OF THE DATA

(a) Total Cross Sections

Using the known theoretical treatment of the deuteron problem (Jankus, Blankenbecler), we shall express our results in the form of Eq. (9). If we use the calculated values of Δ due to Blankenbecler, we may solve for σ_n/σ_p as follows:

$$\frac{\sigma_n}{\sigma_p} = \frac{\sigma_d^{\text{in}}}{\sigma_p} \left(\frac{1}{1+\Delta} \right) - 1, \quad (10)$$

²⁰ R. H. Dalitz and D. R. Yennie, Phys. Rev. **105**, 1598 (1957).

TABLE II. Cross-section ratios.

E (Mev)	θ	σ_d^{in}/σ_p	$(\sigma_n/\sigma_p)_{\Delta=0}$	$(\sigma_n/\sigma_p)_{\Delta\neq 0}$
500	75°	1.22±0.12	0.22±0.12	0.21±0.11
500	90°	1.40±0.24	0.40±0.24	0.39±0.23
500	105°	1.64±0.34	0.64±0.34	0.61±0.30
500	120°	1.57±0.36	0.57±0.36	0.53±0.34
500	135°	1.83±0.30	0.83±0.30	0.80±0.25
600	135°	1.55±0.30	0.55±0.30	...

and σ_d^{in} and σ_p are measured experimentally as shown in Fig. 11. As remarked before, the ratio σ_d^{in}/σ_p in Eq. (10) is independent of the slight error introduced by the thick liquid target. The experimental values of σ_d^{in}/σ_p are given in Table II, as well as values deduced for σ_n/σ_p from Eq. (10) with the appropriate values of Δ . The choice $\Delta=0$ is also made in the table and corresponds to a simple addition of the cross sections [Eq. (4)] without any corrections. Because of the small values of the Δ corrections, the $\Delta=0$ results for σ_n/σ_p are a good approximation to the final result obtained with better values of Δ , calculated by Blankenbecler.

Values of σ_n/σ_p from Table II may now be inserted in Eq. (8), and thus values of F_{2n}^2/F_p^2 may be found for the choices $\Delta=0$ and the Blankenbecler values of Δ . In Fig. 13 the choice $\Delta=0$ is taken and the values of F_{2n}^2 are computed as shown. In this figure the results are presented for F_{2n}^2 and F_p^2 when the proton form factors are modified slightly, as explained above, to fit the Chambers-Hofstadter data. Figure 13 also shows the values of F_{2n}^2 (open circles) when the Blankenbecler values of Δ are inserted. It may be seen that the changes introduced by $\Delta\neq 0$ are not large and within the present experimental errors. In both cases, ($\Delta=0$, $\Delta\neq 0$), the values of F_{2n}^2 lie: (a) on the average, a trifle above the proton form-factor curve, and (b) below the point charge values ($F^2=1.0$) by large amounts. We may conclude immediately, therefore, that (I) the neutron's

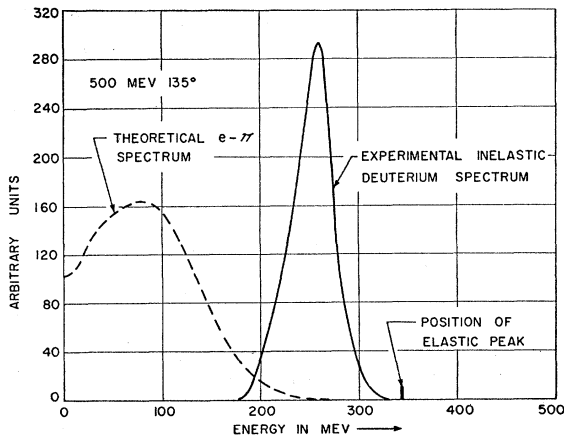


FIG. 12. This figure shows how little the electron-pion peak overlaps the deuteron inelastic continuum, under conditions of greatest overlap in these experiments. The electron-pion spectrum was calculated, using a theory of Dalitz and Yennie¹⁹ and folding their results into the deuteron spectrum.

magnetic radius is not zero or very small ($\sim 2 \times 10^{-14}$ cm), i.e., the neutron is not a point. An equivalent phenomenological statement of this fact is that the neutron's form factor is not unity at the above values of q^2 .

The exact root-mean-square size of the magnetic cloud in the neutron now becomes a matter of prime interest, since we should like to decide whether the cloud has the same dimensions as those of the proton. Phenomenologically speaking, we may state the question in this way: how closely similar are the form factors F_{2n}^2 and F_p^2 ? Both choices, $\Delta=0$, and the Blankenbecler Δ values, show that $F_{2n}^2 \cong F_p^2$. However, the assumption implicit in this statement is that the mesonic exchange contributions to the deuteron electrodisintegration cross section are smaller than about 10%. Because of the good fit of the shapes of the inelastic continua with the Jankus theory (see below), we feel the mesonic effects are rather small. However, if the mesonic corrections prove to be as large as approximately 10% at

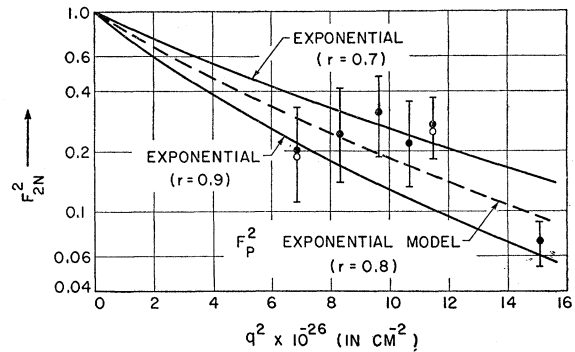


FIG. 13. The dashed line in this figure shows the proton (form factor)² curve, and the solid circles (with experimental limits) show the neutron results of this experiment assuming simple additivity [Eq. (4) or Eq. (10) with $\Delta=0$]. The open circles represent the same data when corrected by the more exact Blankenbecler closure calculations. The changes are slight.

all angles, it can easily be shown that the points in Fig. 13 will fall slightly below the proton curve, and the neutron and proton form factors will not be identical within the errors of this experiment. Thus we may state our second conclusion: (II) If mesonic corrections to deuteron electrodisintegration cross sections are less than approximately 10%, at the q values considered in this experiment, then the neutron's magnetic form factor does not differ from that of the proton, but if the mesonic corrections amount to approximately 10%, the neutron and proton have slightly different magnetic clouds.

If we continue to make the assumption that mesonic effects are small, we may make a determination of the rms size of the neutron. A curved line (exponential model) drawn through unity at $q^2=0$ and the experimental points of Fig. 13 may easily be analyzed to give an rms size of $(0.80 \pm 0.10) \times 10^{-13}$ cm. Thus our third conclusion is as follows: (III) Subject to the assumption that mesonic effects are essentially small, the rms size of

the neutron's magnetic cloud is $(0.80 \pm 0.10) \times 10^{-13}$ cm. It is not possible presently to distinguish a shape factor for the neutron's magnetic cloud, since e.g., within experimental error, both exponential or Gaussian density functions, for a radius of 0.80×10^{-13} cm, can be made to fit the experimental data.

(b) Differential Cross Sections

We shall now give some semi-independent evidence concerning the magnitude of the neutron's form factor. We may use the total cross-section results derived so far as a first approximation to the neutron's form factor, and now we shall consider a potentially more sensitive means of determining the form factor. It has been pointed out by Drell²¹ that if the comparison between the neutron and the proton is carried out by employing the *peak* of the deuteron inelastic continuum and the

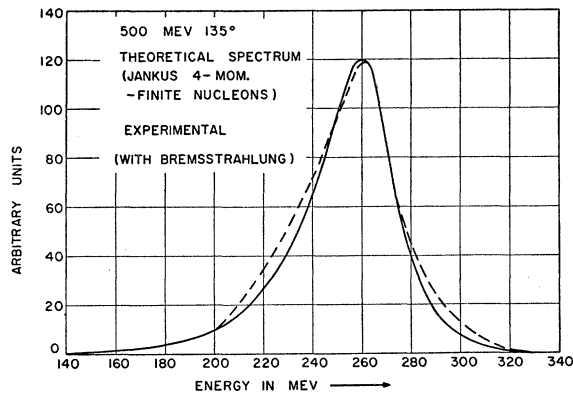


FIG. 14. This figure shows the Jankus four-momentum, finite-nucleon theory at 500 Mev and 135° . Also shown is the experimental spectrum. Bremsstrahlung has been folded into the Jankus theory so that the two curves may be compared directly. The Jankus curve has been adjusted so that its peak value agrees with the experimental curve to facilitate comparison of shape. The wider experimental curve may indicate evidence of small mesonic exchange corrections.

proton's cross section, there is practically no influence on the results due to the previously troublesome mesonic exchange corrections. The reason for this is that in the center-of-mass system there is too little momentum transfer at the deuteron peak to excite the *p*-wave resonance in the pion-nucleon problem. Consequently, we can test and perhaps improve our previous results by comparing the *peak* of the deuteron continuum, rather than its area, with the value of the proton's total cross section.

This test can readily be made by using the experimental curves such as those given in Figs. 3 and 4. The comparison with theory can be accomplished by employing the Jankus result [his Eqs. (9), (10), (11)] with the four-momentum inserted in the equation, in addition to the proton and neutron form factors. The proton form factors are taken from Chambers and

²¹ S. Drell (private communication).

Hofstadter³ and the neutron form factors. We may try to use form factors for the neutron chosen to be equal to those of the proton. In this way, we obtain the new result shown in Fig. 14 at 135° and 500 Mev. The Jankus curve given in that figure represents the improved formulation in which the four-momentum and the form factors are employed and thus represents a deuteron built of finite nucleons. The effects of introducing the form factors are (a) to reduce the ordinate of the point-nucleon curves for the deuteron, as expected from simple considerations, and (b) to widen the theoretical spectrum, because the low-momentum transfers are associated with scattered electrons having energies lower than the peak, where the form factors are higher numerically. The broadening results in improving the agreement of the new curves with experiment, although the experimental curve at 135° is still slightly wider than indicated by theory. The residual width at 135° may represent the effect of mesonic exchange, and, if this is so, we shall have a new way of measuring this correction. In any case, we may compare the actual magnitude of the peak-ordinate of the experimental curve with the peak of the Jankus curve (form factors included). The result is gratifying, for the neutron radius required to give agreement with experiment lies between 0.80×10^{-13} cm and 0.90×10^{-13} cm and is closer to the latter value. For 135° the experimental peak value is 1.51×10^{-34} cm²/sterad Mev, while the theoretical results are 1.90×10^{-34} cm²/sterad Mev for 0.61×10^{-13} cm and 1.49×10^{-34} cm²/sterad Mev for 0.80×10^{-13} cm. The corresponding set of figures for 75° follows: the experimental cross section at the peak is 0.86×10^{-33} cm²/sterad Mev, while the theoretical results are 1.24×10^{-33} cm²/sterad Mev for 0.61×10^{-13} cm and 1.07×10^{-33} cm²/sterad Mev for 0.80×10^{-13} cm. The experimental value at 75° agrees almost exactly with 1.0×10^{-13} cm. At 75° the form-factor curve is similar in shape to the point-nucleon shape except, of course, for the ordinate, which is reduced by the appropriate amount. In view of experimental error, the results show that the peak-comparison-method also gives neutron form factors rather close to those of the proton. Further, the 600 Mev, 135° data are also consistent with size 0.8×10^{-13} cm.

Thus the two methods agree in finding that the neutron's form factors are quite close to those of the proton. The total cross section method favors a slightly smaller size (0.80×10^{-13} cm) and slightly larger form factors, while the method of differential cross sections favors a larger size (0.90×10^{-13} cm) and smaller form factors. We do not know exactly how to weigh these results at the present time. Historically, more effort was devoted to the total cross-section method, although future analyses will also concentrate on the peak-comparison method. If we weigh the two methods equally, the result is $(0.85 \pm 0.10) \times 10^{-13}$ cm for the neutron's magnetic radius, which is equal to the proton's magnetic radius (0.80×10^{-13} cm) within

experimental error (0.10×10^{-13} cm). If the peak-cross-section method is weighed more heavily, the two nucleons have slightly different sizes.

Further work will be devoted to making a sensitive comparison of the neutron and proton by the differential cross-section method. We believe it will be possible, in this way, to test equality of form factors to within a few percent. In addition, the mesonic exchange effects may be investigated by the total cross-section method and by examining the shapes of the inelastic continua.

VI. CONCLUSIONS

We may now summarize the various conclusions which this experiment demonstrates:

(I) The neutron's magnetic cloud is not a point. This result is essentially independent of the various theories which apply to the electrodisintegration process.

(II) The neutron's magnetic form factor is similar to that of the proton. The possible difference between the two form factors is probably not larger than can be represented by the rms sizes of 0.90×10^{-13} cm (neutron) and 0.80×10^{-13} cm (proton).

(III) If mesonic exchange corrections to electrodisintegration are less than 5% or so, the smaller size (0.80) in (II) is suggested for the neutron. If mesonic exchange effects are of the order of 10%, the neutron and proton have slightly different magnetic structures. The results are obtained from the total cross-section method (see text).

(IV) A comparison between neutron and proton made by the differential cross-section method (see text) also indicates that the two nucleons have nearly identical magnetic form factors and identical sizes. By identical, we mean in this context the same to within 10%. This result is consistent with Conclusion III.

(V) The Jankus theory of electrodisintegration of the deuteron appears to be valid beyond the limits within which it was originally developed, provided one uses the four-momentum transfer in its formulas, rather than the three-momentum transfer. Substitution of form factors in the Jankus formulas gives results agreeing remarkably well with experiment. Possible small deviations from theory may be due to mesonic exchange effects.

(VI) Crudely speaking, the results of this experiment are consistent with charge independence. If the results are taken at face value, there is a small difference between the neutron and proton. However, the difference lies within experimental error.

(VII) The question of whether the finite dimensions of the proton¹⁻³ can be ascribed to real structural effects, or whether these dimensions indicate the limits below which quantum electrodynamics may break down, cannot at present be decided uniquely from this experiment. The fact that the Dirac form factor of the proton, the magnetic form factor of the proton, and the magnetic form factor of the neutron all have the same size is suggestive of a common origin, perhaps indicating some limitation of electrodynamics. On the other hand, the small difference that may exist between neutron and proton would suggest structural differences. A more accurate experiment is needed and this is one object of future studies of this type.

(VIII) It is possible that a charge form factor in the neutron could affect the values of F_{2n}^2 , but, since the first and second moments of this distribution vanish, it is unlikely that the above results could be affected in an important manner. Because so little is known about the charge form factor of the neutron, it seems unprofitable to pursue this subject with our present data. On the other hand, Schiff²² has considered this question from a phenomenological point of view.

(IX) In view of the uncertainty in deciding between the total cross-section and differential cross-section methods, the neutron's rms radius may be given as $(0.85 \pm 0.10) \times 10^{-13}$ cm. This radius is consistent with all the conclusions within present experimental error.

ACKNOWLEDGMENTS

We wish to thank Dr. J. A. McIntyre for his help in designing the liquid target and for his assistance in the early stages of working with it. G. Burleson, P. Gram, S. Sobottka, and R. Taylor were also of great help in carrying out the experiment. Dr. F. Bumiller, Dr. H. Ehrenberg, and Dr. H. Kendall generously gave us their aid at various times, particularly with electronic equipment. On the theoretical side, Mr. R. Blankenbecler developed important formulas to interpret our data and we are very grateful to him. Professor S. Drell has pointed out several theoretical features of our problem, which proved to be of fundamental importance and we appreciate his friendly help and advice. We acknowledge with thanks the suggestions of Dr. B. Richter in connection with information on the π^-/π^+ ratio in deuterium. Finally, we wish to thank F. W. Bunker, B. R. Chambers, C. N. Davey, A. Marcum, E. Wright, and Mrs. E. McWhinney for technical assistance.

²² L. I. Schiff, *Bull. Am. Phys. Soc. Ser. II*, **2**, 389 (1957).